Structural and Energetic Analysis of Metal Ions Essential to SRP Signal Recognition Domain Assembly †

2 **AUTHORS**, INCLUDING:

Robert T. Batey
University of Colorado Boulder
85 PUBLICATIONS **4,473** CITATIONS

Structural and Energetic Analysis of Metal Ions Essential to SRP Signal Recognition Domain Assembly[†]

Robert T. Batey[‡] and Jennifer A. Doudna*,[§]

Department of Molecular Biophysics and Biochemistry and Howard Hughes Medical Institute, Yale University, New Haven, Connecticut 06520

Received May 21, 2002; Revised Manuscript Received July 25, 2002

ABSTRACT: The signal recognition particle (SRP) targets proteins to the endoplasmic reticulum in eukaryotes or to the inner membrane in prokaryotes by binding to hydrophobic signal sequences. Signal peptide recognition occurs within the highly conserved RNA−protein core of the SRP, underscoring the importance of this complex in SRP function. Structural analysis of the RNA and protein components of the prokaryotic SRP in the free and bound states revealed that the RNA undergoes a significant conformational change upon protein binding involving the uptake of several monovalent and divalent cations. To investigate the role of these metal ions in formation of the functional SRP complex, we used binding affinity assays and X-ray crystallography to analyze the specificity and energetic contributions of mono- and divalent metal ions bound in the RNA. Our results demonstrate that several metal ion binding sites important for RNA conformation can accommodate chemically distinct ions, often without affecting the structure of the complex. Thus, while these metal ions are highly ordered and essential for the formation and stability of the SRP complex, they behave like nonspecific metal ions.

The signal recognition particle (SRP)[1] is an evolutionarily conserved ribonucleoprotein enzyme that targets proteins for insertion into a cellular membrane or secretion into the extracellular environment (reviewed in ref *1*). In *Escherichia coli*, the SRP is essential for cell viability (*2*) and comprises a single protein, Ffh, bound to the 4.5S RNA (*3*, *4*). During protein synthesis, the SRP binds to a hydrophobic signal sequence on nascent polypeptides destined for the inner membrane, targeting the protein to the membrane in a GTP-dependent process (*5*, *6*). Two functional domains contribute to this activity: the NG domain of the Ffh protein, a Ras-like GTPase (*7*), and the 4.5S RNA−Ffh M domain complex, which is responsible for signal sequence recognition (*8*). The 4.5S RNA contains a universally conserved region of ∼50 nucleotides called domain IV that includes the primary recognition site for the Ffh M domain (*9*, *10*). A truncated version of the 4.5S RNA, including only domain IV, can support growth of an *E. coli* strain conditionally deficient for the 4.5S RNA gene, indicating that this region of the SRP RNA is necessary and sufficient for in vivo function (*11*).

Structures of the individual RNA and protein components of the bacterial SRP determined by NMR and X-ray crystallography, together with the structure of the Ffh M domain−RNA domain IV core complex, revealed that the RNA undergoes a significant conformational change upon binding to the protein (Figure 1a,b) (*11*−*13*). In the complex, a symmetric internal loop and an asymmetric internal loop, each containing nucleotides universally conserved among SRP RNAs, create a unique binding surface for minor groove recognition by the Ffh M domain (Figure 1a). Two non-canonical base pairs in the symmetric loop and a conserved adenosine in the asymmetric loop are energetically critical for interaction with the protein (*11*, *14*). Key nucleotides in the asymmetric loop, tucked into the helix or rotated slightly outward in the free RNA, flip completely out of the helix and stack beneath a universally phylogenetically conserved adenosine residue that binds a pocket on the protein. Modifications of this adenosine are severely detrimental to protein recognition, underscoring the critical importance of the asymmetric internal loop (*15*). Formation of this complex creates a continuous surface comprised of protein and RNA residues that may recognize the hydrophobic and positively charged amino acids within typical signal sequences.

The RNA conformational change essential for SRP assembly and function accompanies the uptake of several monovalent and divalent metal ions that bind to specific sites within domain IV. These ions were observed in the original 1.8 Å resolution crystal structure of the M domain−SRP RNA complex, and their functional importance was suggested by the requirement for potassium and magnesium ions during complex formation (*11*). Since metal ions almost always play a critical role in the biological function of RNA, we set out to unambiguously identify these observed ions and to investigate which were responsible for the structural rearrangement of the SRP RNA. We show here that metal ions lining the major groove of the RNA contribute

---

* To whom correspondence should be addressed. Phone: (510) 643-0225. Fax: (510) 643-0080. E-mail: doudna@uclink.berkeley.edu.

[‡] Present address: Department of Chemistry and Biochemistry, University of Colorado, Boulder, CO 80309.

[§] Present address: Department of Molecular and Cell Biology and Howard Hughes Medical Institute, University of California, Berkeley, CA 94720.

[1] Abbreviations: SRP, signal recognition particle; MES, 2-(4-morpholino)ethanesulfonic acid; MPD, (±)-2-methyl-2,4-pentanediol; HEPES, 4-(2-hydroxyethyl)piperazine-1-ethanesulfonic acid; DTT, 1,4-dithio-DL-threitol.
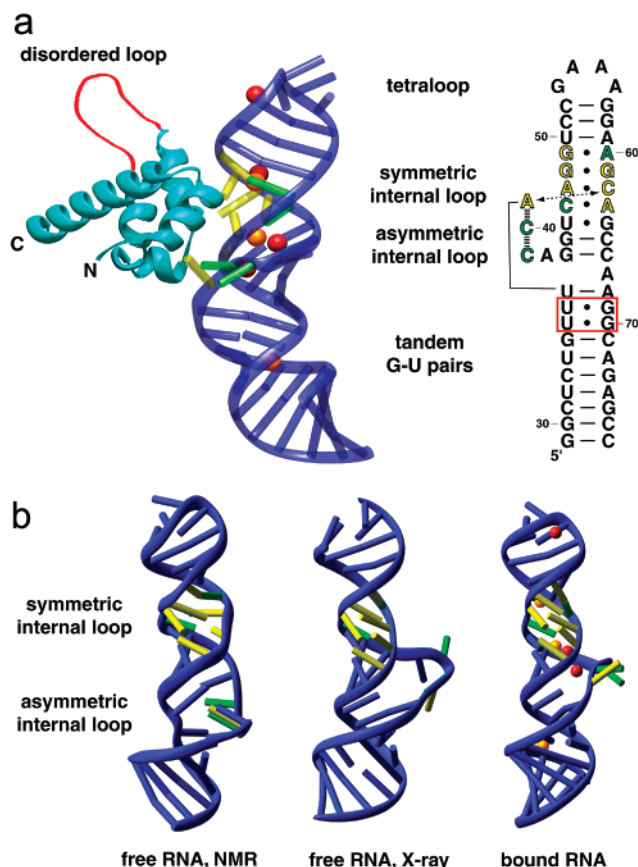
FIGURE 1: (a) Crystal structure of the *E. coli* Ffh M domain−4.5S RNA complex. The M domain (residues 296−453 of Ffh) is represented as a light blue ribbon and the disordered loop (residues 338−370) as a red line. The RNA (containing nucleotides 32−74 of the 4.5S RNA) is depicted as a dark blue ribbon with universally conserved nucleotide bases highlighted in yellow and highly conserved bases in green. Situated within the major groove of the RNA are red and orange spheres, representing, respectively, magnesium and potassium cations that were observed in the refined crystal structure. To the right is a secondary structure diagram of the RNA as observed in the crystal structure. The coloring of the nucleotides corresponds to that in the structure, and the red box encloses the tandem G-U pairs that are a metal binding site. (b) Comparison of the structures of the most phylogenetically conserved domain of the 4.5S RNA in the free and bound forms. While the crystal structures of the free and bound form of the RNA have virtually identical structures in the symmetric internal loop, all three structures differ significantly in the organization of the asymmetric internal loop.

significantly, though indirectly, to protein binding in the RNA minor groove through stabilization of key interactions that form the protein recognition site. Interestingly, however, we find that most of these metal ion binding sites can accommodate chemically distinct cations. While essential for the formation and stability of this RNP, these metal ions display the hallmark of "electrostatically bound" metal ions, as defined by Draper and colleagues (*16*). Within the critical asymmetric internal loop, however, the chemical nature of the divalent cation influences RNA structure and consequently its affinity for the Ffh M domain. These observed effects implicate the metals localized to this region of the RNA as being most critical for protein recognition.

MATERIALS AND METHODS

Materials. The RNAs used in this study were transcribed and purified and proteins expressed using previously pub-

lished protocols (*11*, *14*). The protein construct used for the binding studies is Ffh-M4(C406S), which comprises residues 298−432 of *E. coli* Ffh. This protein binds with the same affinity to the 4.5S RNA as wild-type Ffh as well as Ffh-M2(C406S) that was used for crystallography. The RNA used for the binding studies was the LM10 variant, as described previously (*14*, *15*).

Crystallization of Complexes. The complex that was crystallized contained LM11 RNA and selenomethionine-labeled Ffh-M2(C406S) protein, as described previously (*14*). The protein−RNA complex was prepared for crystallography using a protocol identical to that used previously. For each metal that was investigated, native crystals were first assayed for their ability to be exchanged from the native conditions (200 mM KCl and 10 mM MgCl₂) into a buffer containing the metal ion of interest. Since thallium chloride is insoluble, crystals to be soaked in a thallium-containing solution were grown using a mother liquor containing 50 mM Na-MES (pH 5.6), 200 mM potassium acetate, 10 mM magnesium acetate, and 10% 2-propanol. After the crystals had grown for 2−3 days, the 200 mM potassium acetate was slowly replaced with 200 mM thallium acetate and allowed to incubate for an additional day at 20 °C prior to cryoprotection. A similar soaking protocol using cesium chloride or manganese chloride caused the crystals to rapidly shatter. Therefore, the complex was crystallized under the original conditions, except for the substitution of either 200 mM cesium chloride for potassium chloride or 10 mM manganese chloride for magnesium chloride. The presence of manganese chloride caused excessive nucleation under these conditions, which could be controlled by using a mixture of 120 mM KCl and 80 mM potassium thiocyanate, which yielded moderately large single crystals. Similarly, complexes were grown in the presence of 5 mM cobalt hexamine in place of 10 mM magnesium chloride. All crystals were subsequently cryoprotected by the addition of 30% MPD to the mother liquor and flash-cooled in liquid propane.

Data Collection and Refinement. The structure of each resulting complex was determined by molecular replacement using the program CNS (*17*). The search model that was used was derived from the previously reported structure (PDB entry 1dul) (*11*) by excluding the solvent and metal ions. For the manganese-bound complex, the model was manually rebuilt in the region of A42 and subjected to further rounds of simulated annealing and *B*-factor refinement. Following any manual readjustment of the RNA or protein structure, solvent molecules and metal ions were located in difference Fourier maps contoured at 3σ and built into the structure. The model was then subjected to a further round of simulated annealing and *B*-factor refinement. A summary of data collection and refinement statistics is shown in Table 1.

Equilibrium Binding Assays. Protein−RNA binding assays were performed using a previously described protocol with a few minor modifications (*14*). A constant concentration of 5′-end-labeled RNA (>2 pM) was incubated in a buffer containing 20 mM Tris-HEPES (pH 7.5), 1 mM DTT, 0.01% Igepal-680, and 0.1 mg/mL tRNA along with monovalent and divalent salts. The RNA, after renaturation by heating and cooling, was incubated with protein for at least 1.5 h prior to application to filters. For each experiment, two filters were used: a BA-85 nitrocellulose filter to retain protein−

Table 1: Summary of Crystallographic Data and Refinement

	thallium acetate	cesium chloride	manganese chloride	cobalt hexammine
resolution (Å)	30−2.4	20−2.6	50−2.8	20−1.93
wavelength (Å)	1.5418	1.5418	1.5418	1.5418
no. of unique reflections	13553	10623	8457	28921
total no. of reflections	244654	61945	110349	344199
no. of crystals	5	1	1	4
completeness[a] (%)	98.3 (88.7)	99.2 (98.1)	99.5 (95.9)	95.7 (95.3)
R_{sym}[a,b] (%)	7.8 (35.1)	8.2 (32.5)	10.7 (55.5)	5.0 (34.9)
$I/\sigma(I)$[a]	23.1 (3.5)	16.4 (2.6)	13.5 (2.2)	20.6 (2.3)
R_{cryst} (%)	29.9	29.6	23.6	24.5
R_{free} (%)	32.5	30.3	26.0	25.9

[a] Numbers in parentheses are data for the highest-resolution shell. [b] $R_{sym} = \sum |I - \langle I \rangle| / \sum I$, where I is the observed intensity and $\langle I \rangle$ is the statistically weighted absolute intensity of multiple measurements of symmetry-related reflections.

RNA complexes and a Hybond-N+ nylon membrane to retain free RNA. These filters were soaked in a buffer containing 20 mM Tris-HEPES (pH 7.5) for 1 h prior to use. A 40 μL aliquot from each reaction was applied to the filters and then vacuum applied to draw the samples through the filters. The filters were then briefly air-dried and the free and bound RNA quantified by phosphorimaging.

RESULTS AND DISCUSSION

Specific Metal Ion Uptake Stabilizes SRP Complex Formation. In the crystal structure of the 4.5S RNA alone, metal ions were not observed at any of the binding sites identified in the major groove of the symmetric and asymmetric internal loops in the bound RNA (*11*, *13*). While this may have been a consequence of the high salt concentrations used for crystallization, it is likely that metal ions are taken up by the RNA during SRP complex formation, presumably to stabilize RNA structure and facilitate protein recognition. To determine the specificity of metal ion requirements during formation of the Ffh M domain−4.5S RNA complex, we performed a series of binding affinity measurements in the presence of various monovalent and divalent cations. First, we assayed for the requirement of monovalent and divalent cations in stabilizing the protein−RNA complex (Table 2). These data show that increasing ionic strength significantly facilitates the formation of a high-affinity protein−RNA complex. This contrasts with many protein−nucleic acid interactions, in which increasing ionic strength results in a decrease in binding affinity and a net release of metal ions upon protein binding. An observed decrease in binding affinity as a function of increasing ionic strength indicates formation of electrostatic contacts resulting in counterion release. The opposite trend, reflected in these data, demonstrates that a net uptake of metal ions is an essential aspect of SRP formation. While these measurements were not

carried out at constant ionic strength to probe the relative importance of monovalent versus divalent cations, magnesium ions appear to have the more significant stabilizing influence on the complex. Even at high monovalent cation concentrations, binding of the protein to the RNA is almost 100-fold weaker in the absence of magnesium. Thus, the crystallographically observed divalent and monovalent ions have a strong influence on the stability of the complex. But which of the observed metal ions within the crystal structure might be mediating this effect?

To address this question, we introduced a series of metal ions into the Ffh M domain−RNA complex by cocrystallization or by soaking preformed crystals in a solution containing the metal ion of interest. For each metal ion that was tested, the original crystallization conditions were changed slightly to facilitate the growth of crystals that diffracted to at least 2.8 Å resolution, but these changes did not preclude comparison with native crystals. The structure of each complex that was obtained by soaking or cocrystallization was determined by molecular replacement using the coordinates of the protein and RNA in the native complex; the metals and waters were independently rebuilt for each derivative. In all cases, metal ions were observed in the RNA at four locations: the symmetric internal loop and the asymmetric internal loop that form the protein recognition surface, the flanking GAAA tetraloop, and tandem G-U base pairs.

A Single Low-Specificity Metal Ion Binding Site in the Symmetric Internal Loop. The symmetric internal loop is one of two sites within the 4.5S RNA that directly contacts the M domain of Ffh (*10*, *14*, *18*). The crystal structure of the complex revealed a single magnesium ion in the major groove of this loop (Figure 2a) (*11*, *14*). Manganese substitution produced a strong peak in an anomalous difference electron density map at exactly the location of the magnesium ion in the original model, and a similar result was obtained with cobalt hexammine substitution. Diffraction data from crystals soaked in the presence of thallium or grown in solutions containing cesium produced a strong difference density peak in the major groove side of the symmetric internal loop at the site of one of the inner sphere-coordinated water molecules of the magnesium ion (Figure 2b). These data indicate that this metal ion binding site has a fairly low selectivity for a specific type of monovalent or multivalent ion. In the refined structure of the complex, this is best modeled by assigning half-occupancy to a pentahydrated magnesium ion and half-occupancy to a potassium ion, with the monovalent ion occupying the same position as one of the inner sphere-coordinated waters (*14*). At the salt concentrations used for crystallization, which are similar to physiological conditions (200 mM KCl and 10 mM MgCl$_2$), monovalent and divalent ions probably compete for the same binding site within the major groove of the RNA.

Table 2: Apparent Dissociation Constants[a] (K_d) of the Ffh M4(C406S)-LM10 Complex at 25 °C and Varying Monovalent and Divalent Cation Concentrations

	10 mM MgCl$_2$	100 μM MgCl$_2$	0 mM MgCl$_2$	100 μM MnCl$_2$
200 mM KCl	33 ± 9 pM	220 ± 60 pM	2100 ± 300 pM	20 ± 4 pM
20 mM KCl	47 ± 8 pM	1100 ± 100 pM	>15 μM	100 ± 10 pM
0 mM KCl	87 ± 9 pM	3400 ± 400 pM	nd[b]	220 ± 10 pM

[a] Each value is an average of at least three independent measurements. [b] No detectable binding.
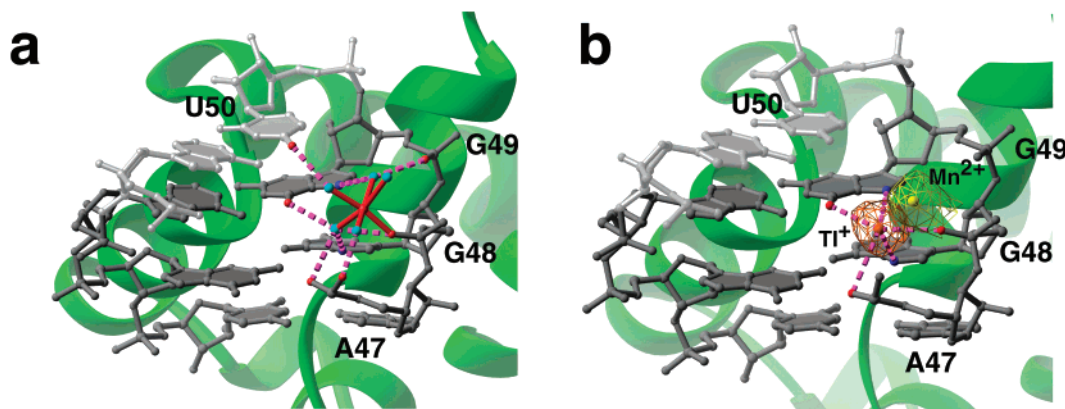
FIGURE 2: Metal ion binding site in the symmetric internal loop of the 4.5S RNA. (a) Within the K^+/Mg^{2+} form of the complex, a magnesium ion is observed within the minor groove of the RNA (in gray; the dark gray highlights the nucleotides in the symmetric internal loop). This magnesium forms a single inner sphere coordination to one of the nonbridging phosphate oxygens of G48, and its inner sphere-coordinated waters (cyan spheres) form extensive hydrogen bonding interactions with the RNA (magenta dashed lines). The protein bound to the minor groove of the RNA is represented as a green ribbon. In the high-resolution structure, the magnesium was modeled with 50% occupancy and a potassium ion, located at the same position as one of the waters, with 50% occupancy. (b) When the crystal was soaked with thallium acetate, there was a clear peak visible in an anomalous difference map (shown as an orange cage), indicating that monovalent ions did bind to that site. This ion was positioned to coordinate N7 and O6 of G49, N7 of G48, and a nonbridging phosphate oxygen of A47 (shown as magenta dashed lines). Crystallizing the complex in manganese chloride yielded clear electron density near the nonbridging oxygen of G48 (yellow cage), indicating the presence of a bound manganese cation.

Interestingly, in the free form of the 4.5S RNA, this site is not occupied by a metal ion; instead, a magnesium ion coordinates to backbone oxygens between A59 and A60 (*13*). Despite this difference, the symmetric internal loop in the two structures is nearly identical (rmsd of 0.72 Å) (*13*). Precise placement of metal ions in the major groove of this loop is thus not essential to formation of the RNA structure recognized by the Ffh M domain.

Conformational Stability of the Asymmetric Internal Loop Involves Specific and Nonspecific Metal Ion Binding Sites. While the symmetric internal loop undergoes little conformational change between the free and bound forms, the asymmetric internal loop exhibits a drastic rearrangement in its structure (Figure 1b). When the RNA goes from the free to the bound form, the bases of the 5′ side of this loop flip out of the helix, presenting the universally conserved base A39 for extensive recognition by the Ffh M domain. The large cavity in the middle of the RNA helix at this site is filled by a well-ordered network of water and metal ions not observed in the free form of the RNA (*11*). In the crystal structure of the complex, a potassium ion positioned in the major groove coordinates to the U45-G64 and C46-A63 pairs (Figure 3, site 1). The identity of this ion was firmly established by the metal ion soaks and cocrystallizations described here. While thallium and cesium exhibited strong peaks of electron density at this position, neither manganese nor cobalt hexammine demonstrated any affinity for this site. Thus, this site appears to be obligatorily a monovalent ion binding site.

The other two metal ion binding sites in the asymmetric loop exhibited a greater diversity in their ability to bind ions. In the structure of the complex crystallized in the presence of cobalt hexammine, only one ammine bound in this loop, near site 3 (Figure 3a,b). This was surprising since this site was occupied by a pentahydrated magnesium ion in the native structure that formed one inner sphere coordination to a nonbridging phosphate oxygen. Site 2, which was occupied by a hexahydrated magnesium ion in the original structure, was instead occupied by a potassium ion. Like the monovalent ion in the symmetric internal loop, it occupied

the position of one of the inner sphere-coordinated waters of the hexahydrated magnesium. This appears to be a general theme at sites that can accommodate both monovalent and divalent cations; the monovalent ion will occupy the position of one of the inner sphere-coordinated waters of the divalent ion. Thus, magnesium primarily interacts with RNA through its inner hydration shell, as observed in recently determined high-resolution tRNA structures (*19*, *20*), while monovalents directly coordinate RNA functional groups, which is their expected behavior based upon a consideration of their differences in the free energies of hydration (*21*). This trend has also been observed in the high-resolution crystal structure of a DNA oligomer at a site in the major groove where there is clear competition between monovalent and divalent cations (*22*).

Crystallization of the complex in the presence of manganese chloride generated another solution to the organization of the asymmetric loop. In the original structure, A42 was flipped out into solution and made a crystal contact with a methionine residue of a neighboring complex. Manganese changed the conformation of this nucleotide by binding to a site within the asymmetric internal loop that allowed it to form inner sphere coordinations with N7 of G43 and one of the nonbridging phosphate oxygens of A42 (Figure 4a). This manganese ion occupies site 3 (Figure 3) in the asymmetric loop, but its exact position is different from that of magnesium or cobalt hexammine, demonstrating that the exact positioning of a metal at this site is strongly dependent upon the nature of the metal. The manganese ion binding to this loop causes A42 to swing into the helix, allowing it to form a *trans*-Hoogsteen sheared A-A pair with A67, the single nucleotide comprising the 3′ side of the asymmetric internal loop (Figure 4b). Consequently, in the presence of manganese, the asymmetric internal loop is converted into a three-nucleotide bulge that still presents the critical A39 to the M domain in exactly the same fashion as observed in the original model. Interestingly, unlike most SRP RNAs that contain four base pairs between the two internal loops that bind the M domain, the *E. coli* 4.5S RNA contains only
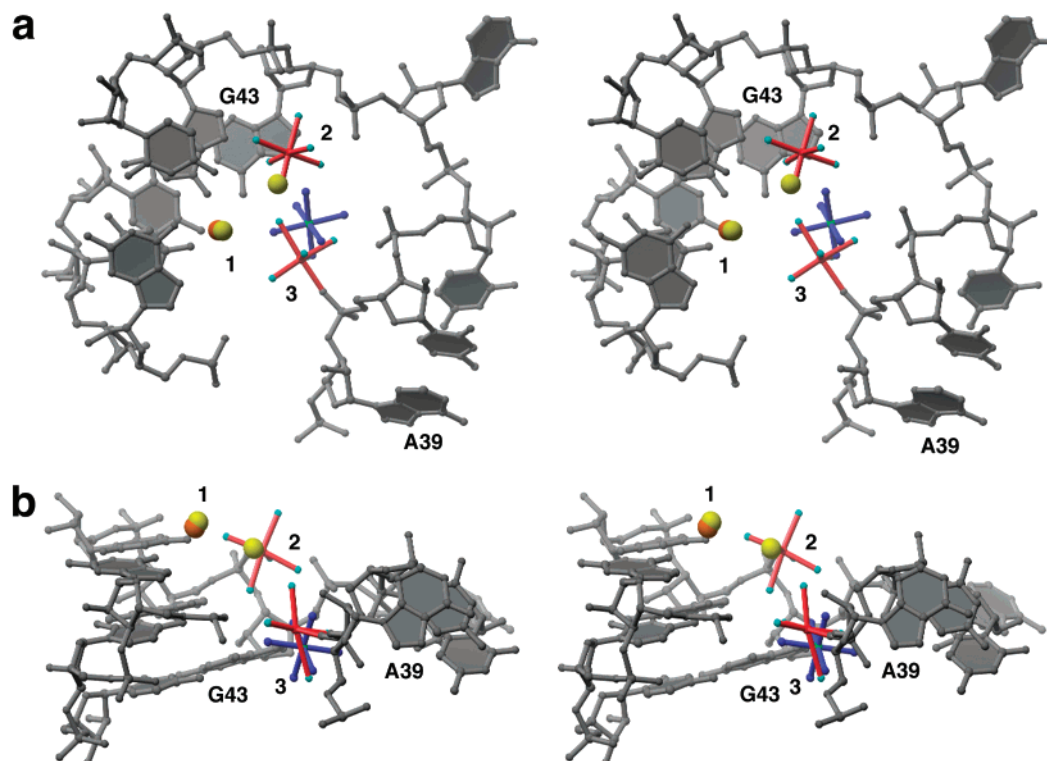
FIGURE 3: Three principal metal ion binding sites in the asymmetric internal loop in the presence of potassium and magnesium (orange and red spheres, respectively) or potassium and cobalt hexammine (yellow and green spheres, respectively). (a) A stereoview looking down the helical axis of the inside of the asymmetric loop and (b) an edge view, highlighting the positions of the metal ions at each of the three principal sites (labeled 1−3). The obligate monovalent ion binding site is labeled 1. Site 2 is occupied by a magnesium ion in the K^+/Mg^{2+} form of the complex and by a potassium ion in the K^+/Co−hexammine complex. Site 3 is occupied by a magnesium ion that forms a single inner sphere coordination with the RNA at one of the nonbridging phosphate oxygens of C40, while cobalt hexammine occupies a slightly different location, allowing its ammine ligands to form a number of hydrogen bonds between O6 and N7 of G43 and the nonbridging phosphate oxygens of C40 and C41.
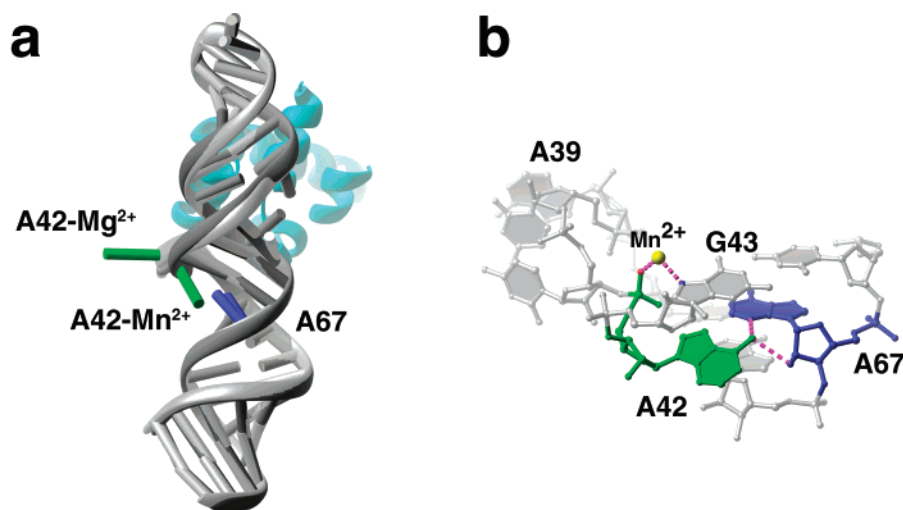

FIGURE 4: Conformational change in the asymmetric internal loop induced in the presence of manganese. (a) The structure of the RNA in the presence of magnesium (light gray) has been superimposed on the structure of the RNA in the presence of manganese. While the single adenosine on the 3′ side of the asymmetric loop (A67) does not significantly change its conformation, A42 (green bar) on the 5′ side of the loop rotates by approximately 90° to form an unusual pair with A67. (b) This conformational change is facilitated by a single manganese ion (yellow sphere) that is observed in the asymmetric loop, positioned to form inner sphere coordinations (purple dashed lines) with N7 of G43 and a nonbridging phosphate oxygen of A42. This allows N6 of A42 to form hydrogen bonds with 2′-OH and N3 of A67 and stack on the sugar of A68.

three base pairs between them (23). The formation of the unusual A-A pair in the presence of manganese, however, creates a fourth pair between the two loops as in all other SRP RNAs. Thus, while crystallized with a divalent cation that is not found at high concentrations physiologically, this structure nonetheless suggests how the asymmetric loop in most other SRP RNAs may be organized.

Like manganese, cesium was able to interact with the asymmetric internal loop in a fashion different from those of the other metals. In the electron density map of the
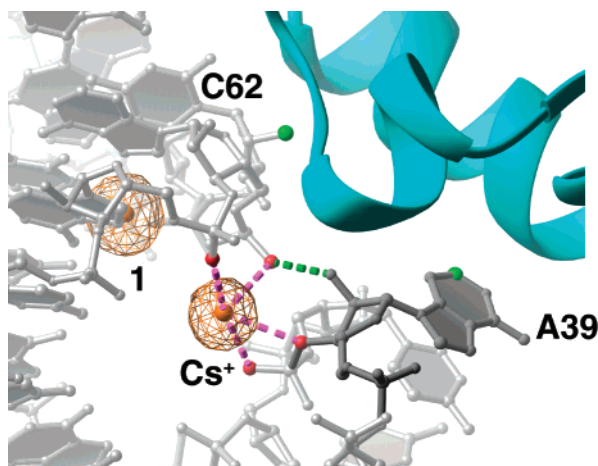
FIGURE 5: Observed cesium ion binding sites in the asymmetric loop. The electron density (orange mesh) represents a 10σ contour level of a $2F_o - F_c$ map of the protein−RNA complex grown in 200 mM cesium chloride. The density at site 1 is cesium bound at the site of monovalent ion binding in the asymmetric internal loop. The other site, denoted Cs^+, represents a cesium ion binding site, coordinated by the nonbridging oxygens of C40, A63, and G64 and O3′ of A39. The distance between each oxygen atom and the cesium ion is 3.1 Å. Two functional groups, 2′-OH of C62 and C2 of A39, near the cesium binding site that are extremely important for protein recognition are highlighted as green balls, and a backbone tertiary contact is shown as a green dashed line.

Table 3: Apparent Dissociation Constants (K_d) of the Ffh M4(C406S)−LM10 Complex at 25 °C and 500 μM Magnesium Chloride

monovalent salt (100 mM)	dissociation constant (pM)[a]
LiCl	980 ± 200
NaCl	210 ± 50
KCl	84 ± 20
RbCl	180 ± 40
CsCl	36 ± 8
NH$_4$Cl	69 ± 11
tetraethylamine chloride	620 ± 40

[a] Each value is an average of at least three independent measurements.

complex crystallized in 200 mM cesium chloride, there was a second site of very high electron density in addition to the potassium site previously described. This occurs at a position where the phosphate backbone of the asymmetric internal loop closely approaches that of the symmetric loop and the 2′-OH of A39 forms a hydrogen bond with the nonbridging phosphate oxygen of A63 (Figure 5). Removal of this hydrogen bond in an RNA mutant containing a deoxyribonucleotide at A39 causes a significant loss of stability of the protein−RNA complex, indicating that this is a necessary structural feature (*15*). A second cesium ion occupies a location near this hydrogen bond, forming four inner sphere coordinations to oxygens in the backbone of the symmetric and asymmetric internal loops (Figure 5). The distances between the cesium ion and each oxygen are ∼3.1 Å, suggesting that smaller monovalent ions would not effectively bridge the two loops. This is consistent with our observation that potassium and thallium do not occupy this site.

These data show that the asymmetric internal loop requires uptake of specific metal ions to stabilize its structure in the bound state. Manganese, which induces a significant conformational change in the loop, also stabilizes the complex more effectively than magnesium at a low concentration (100 μM) (Table 2). The conformation of the asymmetric loop, determined in part by divalent cation identity, directly influences the affinity of the M domain for the 4.5S RNA. Previous work demonstrated that modification of N7 of A63, which forms an inner sphere coordination to the potassium ion in the native structure, is deleterious to protein binding (*11*). Interestingly, when the effect of different monovalent cations upon protein binding was measured, cesium was most effective at stabilizing the complex (Table 3). While potassium and ammonium are generally the most effective monovalent cations for stabilizing RNA tertiary structure

(*24*), the ability of cesium to further stabilize the SRP complex likely reflects its ability to bind to a second site within the asymmetric internal loop (Figure 5). This stabilizes the RNA architecture by screening unfavorable electrostatic interactions that occur where the backbone contacts itself.

Metal Ions Bind the GAAA Tetraloop and Tandem G-U Base Pairs. NMR studies have demonstrated that cobalt hexammine binds to the major groove face of the GAAA tetraloop motif and interacts principally with the first guanosine residue (*25*, *26*). The chemical similarity of the cobalt hexammine ion with hexahydrated magnesium suggested a model for magnesium binding to the tetraloop. In the Ffh M domain−4.5S RNA structure (*11*), a single hexahydrated magnesium ion was observed near the tetraloop (Figure 6a). Three water molecules that are inner sphere-coordinated to the magnesium ion form hydrogen bonds to the O6 and N7 positions of the first guanosine (G53), and to the OP1 and OP2 nonbridging oxygens of the second adenosine (A55). These waters are part of a hydrogen bonding network of highly ordered solvent molecules (labeled a, b, d, and e in Figure 6a) that occupy the major groove face of the tetraloop and coordinate many of the nonbridging phosphate oxygens (highlighted in red). One of these waters (a), was predicted to be part of the GAAA tetraloop motif by Turner and co-workers based upon the thermal stability of this tetraloop and mutants containing functional group substitutions (*27*). Additionally, a recent study of the dynamics of the GAAA tetraloop using fluorescence spectroscopy clearly demonstrated that magnesium and calcium stabilize this motif (*28*). Therefore, it is likely that this solvent network and magnesium ion contribute to the stability of the GAAA motif.

In the structures of the M domain−RNA complex crystallized in the presence of either 5 mM cobalt hexammine or 10 mM manganese chloride, electron density consistent with metal ion binding to the GAAA tetraloop is observed. In the case of cobalt hexammine, however, we observed subtle differences in how the cation interacts with the RNA. While two inner sphere-coordinated ammine ligands interact with O6 and N7 of G53 in a fashion identical to that of magnesium hexahydrate, the OP1 and OP2 nonbridging oxygens of A55 are not contacted by the ammines (Figure 6b). Instead, a water molecule occupies this position, forming hydrogen bonds between cobalt hexammine and a nonbridging phosphate oxygen. The positions of five waters at the major groove (labeled a−e) correspond to the same solvent molecules observed in the magnesium-containing structure. As a consequence of water occupying position c, cobalt hexammine is slightly shifted away from the RNA relative
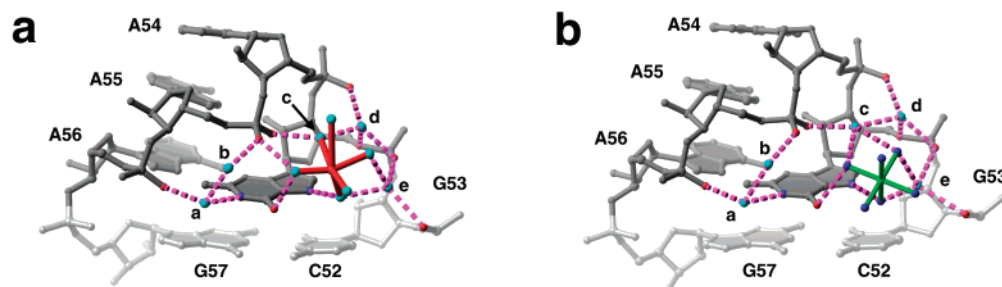
FIGURE 6: Divalent metal ions bound to the major groove face of the GAAA tetraloop. (a) Magnesium hexahydrate (red) bound to the major groove face of the tetraloop. Water molecules that are inner sphere-coordinated to the magnesium ion or are hydrogen bonded to the RNA and are highly ordered are shown as light blue spheres. Five waters that form a hydrogen bonding network of solvent, metal, and RNA are labeled a−e. (b) Cobalt hexammine (green) bound to the major groove face of the tetraloop. Waters occupying the same positions as those labeled a−e in the magnesium form are similarly labeled.
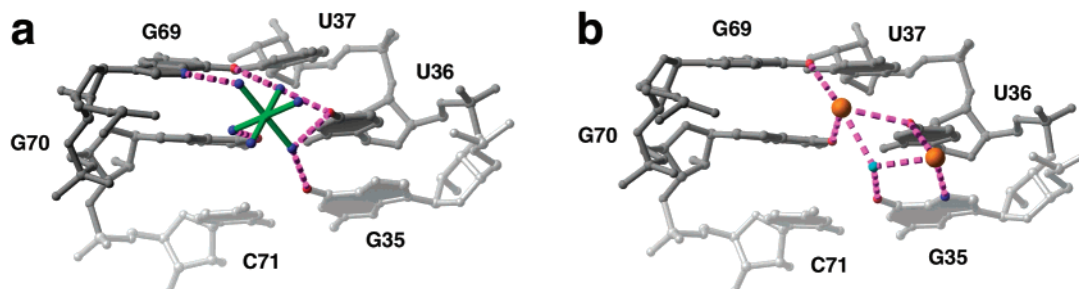

FIGURE 7: Binding of metal ions to tandem G-U pairs in the 4.5S RNA. (a) Binding of a cobalt(III) hexammine ion (green) to tandem G-U pairs. Both a cesium ion and cobalt hexammine interact directly with O2 of U36 and O6 of G69 and G70. (b) Interaction of two cesium ions (orange spheres) with the G-U pairs (represented in dark gray). Coordinations between the cesium ions and the RNA and a well-ordered water (cyan sphere) situated between the ions are represented as magenta dashed lines.

to magnesium hexahydrate. While the cobalt hexammine ion, in this case, occupies the same site as magnesium and manganese hexahydrate, the details of ligand coordination in the RNA are different.

Tandem G-U pairs have been identified previously as sites of metal ion binding in RNA. Within the crystal structure of the P4−P6 domain of the *Tetrahymena thermophila* group I intron, both magnesium ions and hexammines bound to 5′-GG-3′/3′-UU-5′ wobble pairs, while only hexammines bound the 5′-GU-3′/3′-UG-5′ pairs (*29, 30*). That suggests a sequence dependence for the specificity of metal ion binding at this motif. Surprisingly, a 5′-UU-3′/3′-GG-5′ tandem wobble pair in the Ffh M domain−4.5S RNA complex bound a potassium rather than a magnesium ion. Manganese did not bind at this site in anomalous difference electron density maps, supporting the previous observation. However, in the presence of cobalt hexammine, an unambiguous cation was observed in the major groove near the tandem G-U pairs (Figure 7a). Thus, cobalt hexammine is not a perfect analogue of magnesium hexahydrate in that some sites can clearly discriminate between these ions as observed in both the P4−P6 domain and the SRP. This observed difference in the binding of magnesium and cobalt hexammine to RNA has also been observed in a higher-resolution structure of the P4−P6 domain RNA (*31*). Additionally, while thallium substitution produced no identifiable peak in this region, crystallization with cesium revealed two very strong electron density peaks at this site (Figure 7b). Clearly, this type of tandem wobble pair seems to select for monovalent ions and hexammines over divalent cations. While it may in some cases be possible to predict sites of metal ion binding (*32−34*), these data suggest that predicting ion selectivity will be difficult due to the influence of the surrounding sequence.

For example, the cobalt hexammine ion bound at the wobble base pairs in the SRP may be stabilized through interaction with a second cobalt hexammine ion bound to a neighboring site via a chloride ion sandwiched between the two ammines. A recent thermodynamic analysis of magnesium ion binding to various types of tandem G-U pairs also demonstrated that divalent ions do not specifically bind to this motif (*35*).

CONCLUSIONS

Biochemical and crystallographic analysis reveals unexpected properties of metal ion binding sites in the universally conserved domain of the SRP RNA. Metal ion uptake at several sites accompanies high-affinity association of the RNA with the Ffh M domain, yet only one of these sites is selective for a particular ion type. This site, which specifically binds monovalent ions (site 1, Figure 3), occurs in the asymmetric internal loop of the RNA, the region that undergoes a significant conformational change upon protein binding. Its specificity may result from the proximity of three carbonyl functional groups within the major groove of the RNA at this location, similar to the highly specific coordination sites for potassium ions in G-quartet structures and potassium ion channels. Notably, both Cs^+ and Mn^{2+} bind at sites in the asymmetric loop not occupied by K^+/NH_4^+ and Mg^{2+}, respectively, and stabilize the extrahelical positioning of loop nucleotides that is essential to the RNA−protein interaction. The fact that Cs^+ and Mn^{2+} significantly increase the protein−RNA binding affinity over that observed in the presence of K^+ and Mg^{2+} suggests that sites in the asymmetric loop of the RNA are primarily responsible for the metal ion-dependent stabilization of the SRP complex.

Despite the importance of metal ion binding sites for RNA folding and function, identifying and characterizing them

within RNA molecules remain a challenge. The observed sites of metal binding in RNA crystal structures are highly dependent on the identity and concentration of ions used during crystallization. Computer algorithms that use surface potential calculations (*33, 34*) or Brownian dynamics simulations (*32*) of an RNA molecule can predict approximate locations but not specificities of likely metal ion binding sites. On the basis of the results of this study, many of these observed and predicted sites in RNA may have a surprisingly broad specificity for cations that may prove to be difficult to model. To be able to predict ion binding specificities for each modeled site, computer simulations would need to be able to account for the chemical nature of the ion, functional groups in the RNA that surround the ion binding site, the water structure around the nucleic acid, and conformational changes in RNA. Only a detailed structural and biochemical analysis of metal−RNA interactions using a diverse set of monovalent and divalent cations can reveal a complete picture of this critical aspect of RNA structure.

ACKNOWLEDGMENT

REFERENCES

1. Keenan, R. J., Freymann, D. M., Stroud, R. M., and Walter, P. (2001) The signal recognition particle, *Annu. Rev. Biochem. 70*, 755−775.
2. Phillips, G. J., and Silhavy, T. J. (1992) The *E. coli ffh* gene is necessary for viability and efficient protein export, *Nature 359*, 744−746.
3. Poritz, M. A., et al. (1990) An *E. coli* ribonucleoprotein containing 4.5S RNA resembles mammalian signal recognition particle, *Science 250*, 1111−1117.
4. Ribes, V., Römisch, K., Giner, A., Dobberstein, B., and Tollervey, D. (1990) *E. coli* 4.5S RNA is part of a ribonucleoprotein particle that has properties related to Signal Recognition Particle, *Cell 63*, 591−600.
5. de Gier, J.-W. L., et al. (1996) Assembly of a cytoplasmic membrane protein in *Escherichia coli* is dependent on the signal recognition particle, *FEBS Lett. 399*, 307−309.
6. Ulbrandt, N. D., Newitt, J. A., and Bernstein, H. D. (1997) The *E. coli* signal recognition particle is required for the insertion of a subset of inner membrane proteins, *Cell 88*, 187−196.
7. Freymann, D. M., Keenan, R. J., Stroud, R. M., and Walter, P. (1997) Structure of the conserved GTPase domain of the signal recognition particle, *Nature 385*, 361−364.
8. Zopf, D., Bernstein, H. D., Johnson, A. E., and Walter, P. (1990) The methionine-rich domain of the 54 kda protein subunit of the signal recognition particle contains an RNA binding site and can be crosslinked to a signal sequence, *EMBO J. 9*, 4511−4517.
9. Lentzen, G., Moine, H., Ehresmann, C., Ehresmann, B., and Wintermeyer, W. (1996) Structure of 4.5S RNA in the signal recognition particle of *Escherichia coli* as studied by enzymatic and chemical probing, *RNA 2*, 244−253.
10. Schmitz, U., et al. (1996) NMR studies of the most conserved RNA domain of the mammalian signal recognition particle (SRP), *RNA 2*, 1213−1227.
11. Batey, R. T., Rambo, R. P., Lucast, L., Rha, B., and Doudna, J. A. (2000) Crystal structure of the ribonucleoprotein core of the signal recognition particle, *Science 287*, 1232−1239.
12. Schmitz, U., et al. (1999) Structure of the phylogenetically most conserved domain of SRP RNA, *RNA 5*, 1419−1429.
13. Jovine, L., et al. (2000) Crystal structure of the ffh and EF-G binding sites in the conserved domain IV of *Escherichia coli* 4.5S RNA, *Folding Des. 8*, 527−540.
14. Batey, R. T., Sagar, M. B., and Doudna, J. A. (2001) Structural and energetic analysis of RNA recognition by a universally conserved protein from the signal recognition particle, *J. Mol. Biol. 307*, 229−246.
15. Doherty, E. A., Batey, R. T., Masquida, B., and Doudna, J. A. (2001) A universal mode of helix packing in RNA, *Nat. Struct. Biol. 8*, 339−343.
16. Misra, V. K., and Draper, D. E. (1998) On the role of magnesium ions in RNA stability, *Biopolymers 48*, 113−135.
17. Brünger, A. T., et al. (1998) Crystallography & NMR system: A new software suite for macromolecular structure determination, *Acta Crystallogr. D54*, 905−921.
18. Lentzen, G., Dobberstein, B., and Wintermeyer, W. (1994) Formation of SRP-like particle induces a conformational change in *E. coli* 4.5S RNA, *FEBS Lett. 348*, 233−238.
19. Shi, H., and Moore, P. B. (2000) The crystal structure of yeast phenylalanine tRNA at 1.93 Å resolution: a classic structure revisited, *RNA 6*, 1091−1105.
20. Jovine, L., Djordjevic, S., and Rhodes, D. (2000) The crystal structure of yeast phenylalanine tRNA at 2.0 Å resolution: cleavage by Mg^{2+} in 15-year-old crystals, *J. Mol. Biol. 301*, 401−414.
21. Draper, D. E., and Misra, V. K. (1998) RNA shows its metal, *Nat. Struct. Biol. 5*, 927−930.
22. Howerton, S. B., Sines, C. C., VanDerveer, D., and Williams, L. D. (2001) Locating monovalent cations in the grooves of B-DNA, *Biochemistry 40*, 10023−10031.
23. Gorodkin, J., Knudsen, B., Zweib, C., and Samuelsson, T. (2001) SRPDB (Signal Recognition Particle Database), *Nucleic Acids Res. 29*, 169−170.
24. Shiman, R., and Draper, D. E. (2000) Stabilization of RNA tertiary structure by monovalent cations, *J. Mol. Biol. 302*, 79−91.
25. Maderia, M., Horton, T. E., and DeRose, V. J. (2000) Metal interactions with a GAAA RNA tetraloop characterized by ^{31}P NMR and phosphorthioate substitutions, *Biochemistry 39*, 8193−8200.
26. Rüdisser, S., and Tinoco, I., Jr. (2000) Solution structure of cobalt-(III)hexammine complexed to the GAAA tetraloop, and metal-ion binding to G·A mismatches, *J. Mol. Biol. 295*, 1211−1223.
27. SantaLucia, J., Jr., Kierzek, R., and Turner, D. H. (1992) Context dependence of hydrogen bond free energy revealed by substitutions in an RNA hairpin, *Science 256*, 217−219.
28. Menger, M., Eckstein, F., and Porschke, D. (2000) Dynamics of the RNA hairpin GNRA tetraloop, *Biochemistry 39*, 4500−4507.
29. Kieft, J. S., and Tinoco, I. J. (1997) Solution structure of a metal-binding site in the major groove of RNA complexed with cobalt-(III) hexammine, *Structure 5*, 713−721.
30. Cate, J. H., and Doudna, J. A. (1996) Metal-binding sites in the major groove of a large ribozyme domain, *Structure 4*, 1221−1229.
31. Juneau, K., Podell, E., Harrington, D. J., and Cech, T. R. (2001) Structural basis of the enhanced stability of a mutant ribozyme domain and a detailed view of RNA-solvent interactions, *Structure 9*, 221−231.
32. Auffinger, P., and Westhof, E. (2000) Water and ion binding around RNA and DNA (C,G) oligomers, *J. Mol. Biol. 300*, 1113−1131.
33. Chin, K., Sharp, K. A., Honig, B., and Pyle, A. M. (1999) Calculating the electrostatic properties of RNA provides new insights into molecular interactions and function, *Nat. Struct. Biol. 6*, 1055−1061.
34. Misra, V. K., and Draper, D. E. (2000) Mg^{2+} binding to tRNA revisited: the nonlinear Poisson−Boltzmann model, *J. Mol. Biol. 299*, 813−825.
35. Serra, M. J., et al. (2002) Effects of magnesium ions on the stabilization of RNA oligomers of defined structures, *RNA 8*, 307−323.